Synthesis of 1,4-phenylene-bridged linear porphyrin arrays

Atsuhiro Osuka,* Nobuhiro Tanabe, Satoshi Nakajima and Kazuhiro Maruyama

Department of Chemistry, Faculty of Science, Kyoto University, Kyoto 606, Japan

1,4-Phenylene-bridged, linear porphyrin arrays including the dimer, trimer, pentamer, heptamer and nonamer have been synthesized by acid-catalysed condensation of formyl-substituted porphyrins with bis(3-ethyl-4-methylpyrrol-2-yl)methane in moderate yields. The molecular length of the nonamer is estimated to be as long as *ca.* 122 Å. The Soret bands of both zinc complexes and doubly protonated free base porphyrins are split depending upon the number of the porphyrins, which can be explained in terms of exciton coupling theory. With an increase in the number of the porphyrins, the fluorescence spectra become broader and red-shifted without significant decrease in the fluorescence quantum yield, reflecting their stretched conformations that do not allow the formation of a singlet-excitation-energy trapping site.

Photosynthetic organisms use light-harvesting complexes to capture sunlight and funnel the energy to the reaction centre. Efficient energy transfer of these light-harvesting complexes, which occurs over long-distances and involves hundreds of chromophores, must be related to their highly ordered array of photosynthetic pigments. Recent remarkable success in elucidation of the three dimensional structure of the light-harvesting complex (LH2) from a photosynthetic bacterium[1] highlights the importance of regularly arranged chromophore arrays. Understanding light-harvesting phenomena at the molecular level has been aided by studies on synthetic porphyrin-based model systems.[2] Covalent arrays of five or more porphyrins with well-defined geometries are essential for probing the effects of molecular organization on chromophoric interactions and energy migration processes.[3-8]

In earlier work, we reported the synthesis of linear and stacked porphyrin trimers and pentamers,[3b] which are substituted in the β-positions with methyl and ethyl groups. Upon increasing the number of porphyrin rings, we faced a serious solubility problem, which hampers manipulation of higher homologues. It was thought that replacement of the peripheral substituents would yield solubility enhancement such that longer porphyrin arrays could be manipulated in common organic solvents. In this paper, we report the synthesis of linear, 1,4-phenylene-bridged porphyrin arrays **1**–**6** which are substituted with methyl and hexyl substituents in most of the β-positions and with 3,5-di-*tert*-butylphenyl groups[9] in the terminal meso-positions.

Results and discussion

The synthetic strategy is quite simple. First, formyl-substituted porphyrin monomer **7** was prepared in 37% yield from the condensation of 3,5-di-*tert*-butylbenzaldehyde **11** and 4-(5,5-dimethyl-1,3-dioxacyclohexan-2-yl)benzaldehyde **12** with bis(3-hexyl-4-methylpyrrol-2-yl)methane **13**[10] followed by oxidation with *p*-chloranil and subsequent hydrolysis of the acetal protecting group with trifluoroacetic acid (TFA). Formyl-substituted porphyrin dimer **8**, trimer **9** and tetramer **10** were prepared by the reaction of **7**, **8** and **9** with **12** and **13** in essentially the same manner in 49, 42 and 48% yields, respectively. The final homocondensation of **7**, **8**, **9** and **10** with bis(3-ethyl-4-methylpyrrol-2-yl)methane **14**[11] followed by oxidation with *p*-chloranil afforded symmetric porphyrin arrays, trimer **3** (47%), pentamer **4** (37%), heptamer **5** (16%) and nonamer **6** (38%), respectively. The yields were not optimized. Use of **13** instead of **14** in the final step led to lower yields; the yields of the corresponding trimer **3′**, pentamer **4′** and heptamer **5′** were 17, 19 and 8%, respectively. Porphyrin monomer **1** and dimer **2**[3d] were also prepared as reference compounds. The porphyrin arrays **3**–**6** are all quasi-one-dimensional and laterally 44, 70, 96 and 122 Å long, respectively, on the basis of CPK models. To the best of our knowledge, **6** is the longest porphyrin oligomer ever prepared. Since the meso-aryl substituents are held nearly perpendicular to the porphyrin plane owing to the steric hindrance between the aryl substituents and the flanking methyl groups, all the porphyrins in these arrays can be regarded as being held in a regular coplanar arrangement.

These porphyrin arrays have been characterized by their 500 MHz ^{1}H NMR spectra and FAB mass spectra. Satisfactorily resolved ^{1}H NMR spectra were obtained for **1**–**3** in $CDCl_3$ but poor solubility precluded the measurement of higher oligomers **4**–**6**. We found that these oligomeric porphyrins dissolved in [^{2}H]TFA, probably as fully protonated forms. Fig. 1 shows the ^{1}H NMR spectra of **1**, **2**, **3′**, **4′**, **5′** and **6** taken in [^{2}H]TFA. The spectra indicated their good purities. Upon the increase of the number of porphyrin rings, the spectra became increasingly broader, reflecting the effect of molecular size. However, the respective chemical shifts were virtually unchanged from the dimer to the nonamer, indicating similar environments of the respective porphyrins. The porphyrin arrays all gave satisfactory positive FAB-MS consistent with the assigned structures (see Experimental section).

The absorption and fluorescence spectra of the zinc complexes of **1**–**6** in THF are presented in Figs. 2 and 3. Other than **1**, all the zinc porphyrin oligomers displayed split Soret bands owing to the exciton coupling. The Soret bands at shorter wavelength are observed at nearly the same wavelength (*ca.* 416 nm), while those at longer wavelength shift steadily to longer wavelength upon the increase of the number of the porphyrins. The relative intensities of the split Soret bands also depend on the number of the porphyrins; the intensity of longer wavelength bands become increasingly stronger relative to that at the shorter wavelength. These split Soret bands were deconvoluted into two Gaussian curves, from which we determined the exciton coupling energy ΔE. According to the simple theory of the exciton coupling,[12] we can expect the relationship of eqn. (1), where E_0 is the exciton coupling energy

$$\Delta E = 2E_0 \cos[\pi/(N + 1)] \qquad (1)$$

between the neighbouring porphyrins and N is the number of the porphyrins. Therefore, we plotted these data according to

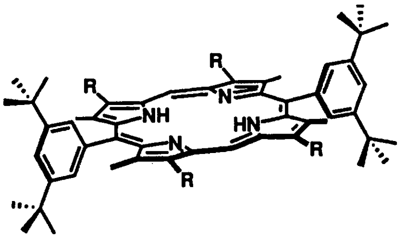

1

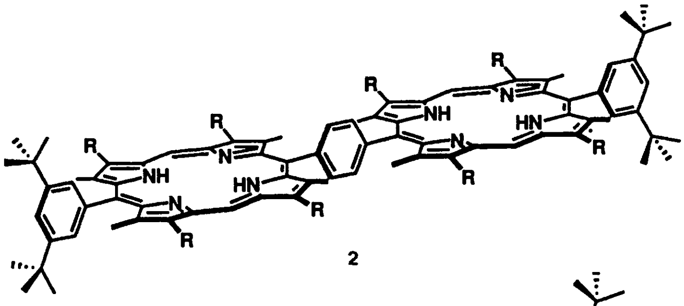

2

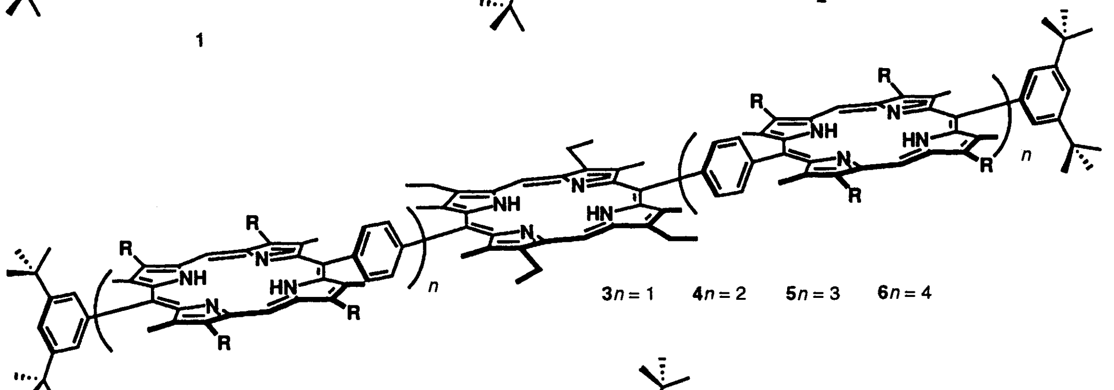

3 $n = 1$ 4 $n = 2$ 5 $n = 3$ 6 $n = 4$

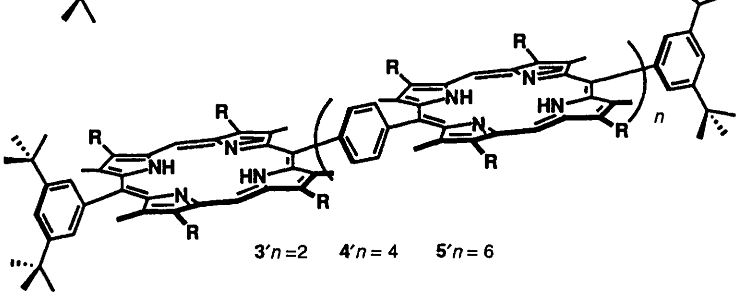

3′ $n = 2$ 4′ $n = 4$ 5′ $n = 6$

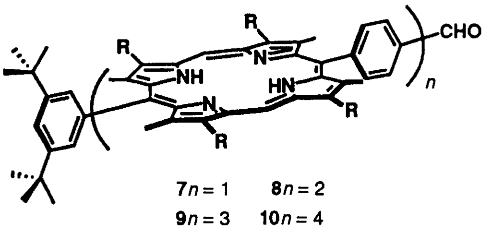

7 $n = 1$ 8 $n = 2$

9 $n = 3$ 10 $n = 4$

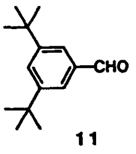

11

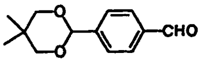

12

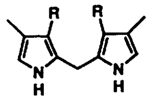

13 R = C_6H_{13}

14 R = C_2H_5

eqn. (1) (Fig. 4). In accord with the previous study,[3b] a good linear relationship was observed for up to the heptamer **5(Zn$_7$)** but the plot of the nonamer **6(Zn$_9$)** deviates markedly. At a glance, the spectral shape of **6(Zn$_9$)** differs substantially from those of **2(Zn$_2$)**–**5(Zn$_7$)**. It is conceivable that the nonamer **6(Zn$_9$)** tends to aggregate more extensively than **2(Zn$_2$)**–**5(Zn$_7$)** even at the low concentration of *ca.* 3×10^{-7} mol dm^{-3}, which may lead to the observed spectral change. On the other hand, the fluorescence spectra recorded for these zinc complexes exhibit rather systematic changes (Fig. 3): the fluorescence peak maxima are shifted to longer wavelength and the spectral bands become increasingly broader. Characteristic vibrational bands observed for **1(Zn)** change to a broad, nearly one-peaked band for **6(Zn$_9$)**. It may be notable that even for the heptamer or nonamer, the relative fluorescence intensity does not decrease so significantly. These results are consistent with constrained, stretched conformations of these porphyrin arrays that do not allow the formation of excitation-energy trapping sites such as closely interacting dimers.

Fig. 5 shows the absorption spectra of these porphyrin arrays **1**–**6** in TFA, in which all the porphyrins should exist as doubly protonated forms that will induce disaggregation owing to electrostatic repulsion. Under these conditions, we observed rather systematic change of the absorption spectra both in the Soret- and Q-band regions. When the split Soret bands were analysed similarly in terms of eqn. (1), we obtained a better linear plot including a point for the nonamer as shown in Fig. 4 with a slope of $E_0 = 1200$ cm^{-1}, which is larger than a value of 800 cm^{-1} for the zinc series. These results indicate that all the porphyrins in these arrays are aligned in regular arrangements in the fully protonated forms, as we may expect from paper-drawn structures. The larger E_0 value for the dication in comparison to that for the zinc complex can be understood in terms of larger oscillator strength of the Soret band of the dication. Upon the increase in the numbers of porphyrin, the fluorescence spectra do not show a decreasing tendency in their relative intensity but display an inverse increasing tendency of **1** < **2** < **3** < **4** and the fluorescence intensities of **4**, **5** and **6** are roughly the same (Fig. 6). These results again indicate the lack of an energy-trapping site in these protonated porphyrin arrays.

In summary, our synthetic method for 1,4-phenylene-bridged oligomeric porphyrin arrays has been successfully extended to give a porphyrin heptamer and nonamer by introducing appropriate peripheral and terminal aryl substituents. The porphyrin arrays reported here will be very useful for studying repeated energy hopping processes over the regularly arranged pigments and for studying multiple chromophoric interactions. Studies directed toward preparing even longer porphyrin arrays and examination of long-range energy transfer across these supramolecular arrays are in progress by preparing models in which energy donors and acceptors are covalently attached to these linear porphyrin arrays.

Experimental

All solvents and reagents were purified by standard methods before use. The instruments were as previously reported.[10] ^{1}H NMR spectra were taken on a 500 MHz JEOL α-500 spectrometer, and coupling constants (*J*) are given in Hz. In the assignments of the resonances, Hex-1–Hex-6 refer to protons on the 1–6 position, respectively, of the hexyl substituents. Mass spectra were recorded on a JEOL HX-100 spectrometer using the positive FAB ionization method (accelerating voltage

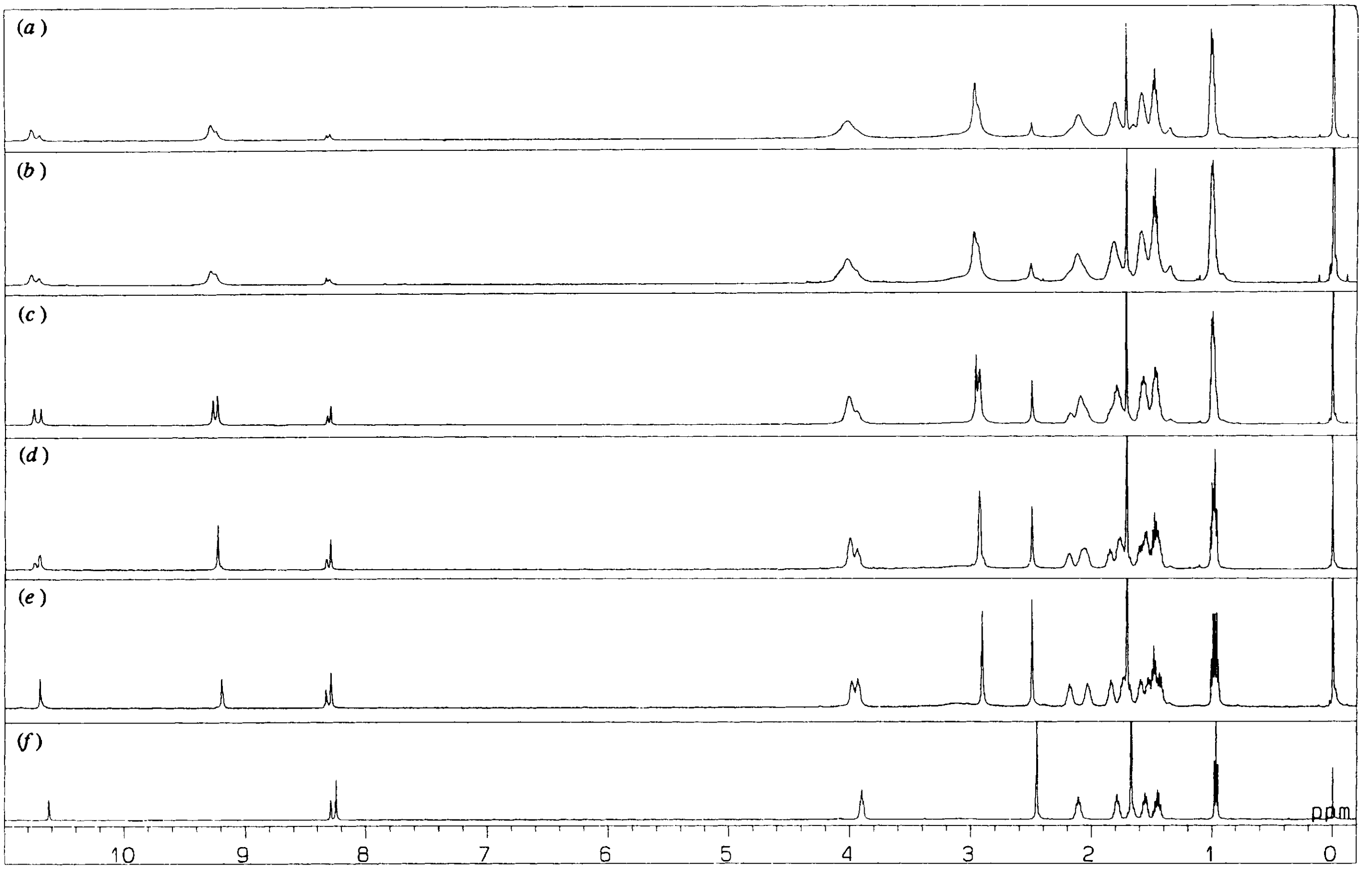

Fig. 1 500 MHz ^{1}H NMR spectra taken in [^{2}H]TFA; (*a*) **6**, (*b*) **5′**, (*c*) **4′**, (*d*) **3′**, (*e*) **2** and (*f*) **1**

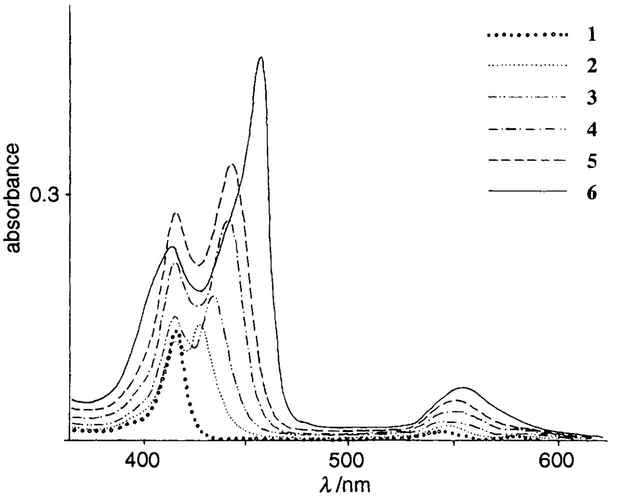

Fig. 2 Absorption spectra of zinc complexes of **1**–**6** taken in THF; concentrations are 3 × 10^{-7} mol dm^{-3}

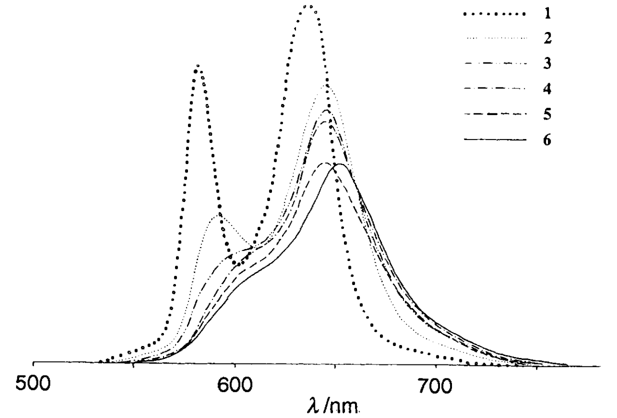

Fig. 3 Steady-state fluorescence spectra for zinc complexes of **1**–**6** taken in THF for excitation at 416 nm, at which the absorbances were adjusted *ca.* 0.2

10 kV, Xe atom as the primary ion source, and a mixture of 3-nitrobenzyl alcohol–$CHCl_3$ as the FAB matrix).

Preparation of formyl substituted linear porphyrins

Aldehydes **11** (545 mg, 2.5 mmol) and **12**[10] (550 mg, 2.5 mmol) were dissolved in dry MeCN (50 cm^3). Then, dipyrrylmethane **13**[10] (1710 mg, 5 mmol) dissolved in MeCN (5 cm^3) was added. The resulting solution was stirred for 2–3 min and then trichloroacetic acid (TCA) (60 mg, 0.37 mmol) in dry MeCN (3 cm^3) was added. The mixture was stirred at room temp. overnight under N_2 in the dark. A solution of *p*-chloranil (1.8 g) in dry THF (60 cm^3) was added, and stirring was continued for another 3 h. The resulting reaction mixture was poured into 6 mol dm^{-3} HCl solution and extracted with $CHCl_3$ until the extract was colourless. The $CHCl_3$ layers were combined,

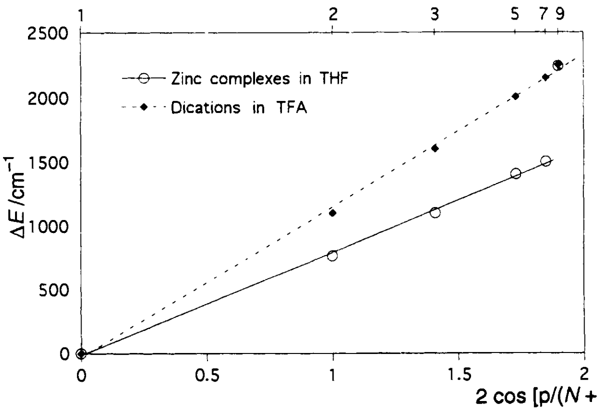

Fig. 4 Plots of excitation splitting energy *versus* 2 cos[π(*N* + 1)]

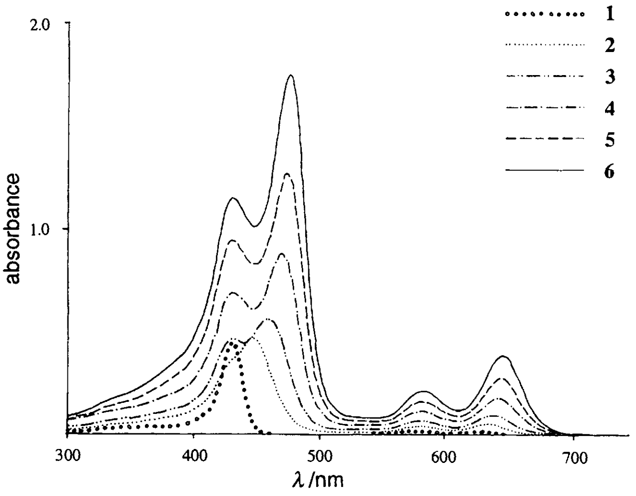

Fig. 5 Absorption spectra of zinc complexes of **1**–**6** taken in TFA; concentrations are 1 × 10^{-6} mol dm^{-3}

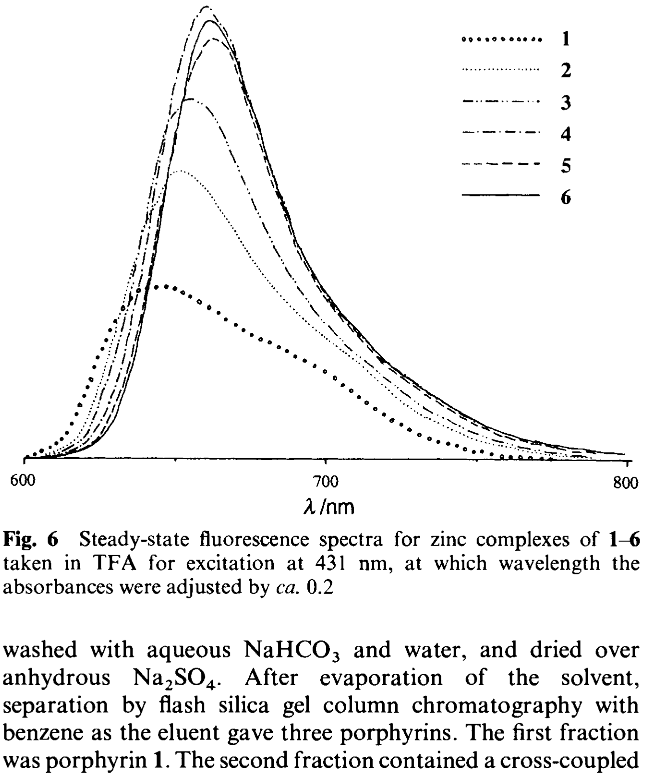

Fig. 6 Steady-state fluorescence spectra for zinc complexes of **1**–**6** taken in TFA for excitation at 431 nm, at which wavelength the absorbances were adjusted by *ca.* 0.2

washed with aqueous $NaHCO_3$ and water, and dried over anhydrous Na_2SO_4. After evaporation of the solvent, separation by flash silica gel column chromatography with benzene as the eluent gave three porphyrins. The first fraction was porphyrin **1**. The second fraction contained a cross-coupled porphyrin product. After evaporation of the solvent, the residue was dissolved in a mixture of CH_2Cl_2 (100 cm^3), TFA (100 cm^3) and water (20 cm^3). After refluxing for 3 h, the resulting mixture was poured into ice–water and extracted with $CHCl_3$ (3 × 100 cm^3). The $CHCl_3$ layers were combined, successively washed with aqueous $NaHCO_3$ and water, and dried over anhydrous Na_2SO_4. Recrystallization from CH_2Cl_2 and methanol gave **7** (923 mg, 37% based on the amount of **13** used).

Formyl substituted porphyrins **8**, **9** and **10** were prepared in the similar manner with some modifications: firstly, the ratio of formyl substituted porphyrin to **12** was 3–5 and secondly, the dipyrrylmethane **13** was added to a homogeneous solution of the formyl-substituted porphyrin **12** and TCA in a mixture of CH_2Cl_2 and MeCN. The preparation of **8** was typical. To a solution of **7** (1297 mg, 1.3 mmol), **12** (858 mg, 3.9 mmol) and TCA (595 mg, 3.64 mmol) in CH_2Cl_2 (40 cm^3) and MeCN (156 cm^3), was added a solution of **13** (1778 mg, 5.2 mmol) in MeCN (39 cm^3). Use of excess TCA is critical in achieving a high yield. After the same work-up, formyl substituted porphyrin **8** was obtained (1127 mg, 49% yield based on the amount of **7** used).

Formyl-substituted monomer 7. $\delta_H(CDCl_3)$ 10.40 (1 H, s, CHO), 10.24 (2 H, s, 2 × mesoH), 8.29 (4 H, dd, *J* 7.8 and 7.8, 4 × ArH), 7.91 (2 H, d, *J* 1.5, 2 × ArH), 7.81 (1 H, t, *J* 1.5, ArH), 3.98 (8 H, t, *J* 8.1, 4 × Hex-1), 2.46 (12 H, s, 4 × Me), 2.17 (8 H, m, 4 × Hex-2), 1.72 (8 H, m, 4 × Hex-3), 1.50 (18 H, s, 2 × Bu^t), 1.47 (8 H, m, 4 × Hex-4), 1.35 (8 H, m, 4 × Hex-5), 0.90 (6 H, t, *J* 7.3, 2 × Hex-6), 0.89 (6 H, t, *J* 7.3, 2 × Hex-6), −2.39 (2 H, br, 2 × NH); *m*/*z* 996 (calc. 995 for $C_{69}H_{94}N_4O$).

Formyl-substituted dimer 8. $\delta_H(CDCl_3)$ 10.39 (1 H, s, CHO), 10.36 (2 H, s, 2 × mesoH), 10.34 (2 H, s, 2 × mesoH), 8.53 (4 H, dd, *J* 7.8 and 7.8, 4 × ArH), 8.27 (4 H, dd, *J* 7.8 and 7.8, 4 × ArH), 7.95 (2 H, d, *J* 2.0, 2 × ArH), 7.83 (1 H, t, *J* 2.0, ArH), 4.15 (8 H, t, *J* 8.1, 4 × Hex-1), 4.03 (8 H, t, *J* 7.8, 4 × Hex-1), 3.18 (12 H, s, 4 × Me), 2.50 (6 H, s, 2 × Me), 2.48 (6 H, s, 2 × Me), 2.34–2.24 (16 H, m, 8 × Hex-2), 1.90–1.73 (16 H, m, 8 × Hex-3), 1.60–1.50 (16 H, m, 8 × Hex-4), 1.53 (18 H, s, 2 × Bu^t), 1.47–1.37 (16 H, m, 8 × Hex-5), 0.96 (12 H, t, *J* 7.4, 4 × Hex-6), 0.94 (6 H, t, *J* 7.4, 2 × Hex-6), 0.93 (6 H, t, *J* 7.4, 2 × Hex-6), −1.78 (2 H, br, 2 × NH), −2.02 (2 H, br, 2 × NH); *m*/*z* 1772 (calc. 1772 for $C_{123}H_{166}N_8O$).

Formyl-substituted trimer 9. $\delta_H(CDCl_3$, HCl salt) 10.46 (1 H, s, CHO), 10.36 (2 H, s, 2 × mesoH), 10.33 (2 H, s, 2 × mesoH), 10.32 (2 H, s, 2 × mesoH), 8.94 (8 H, m, 8 × ArH), 8.50 (4 H, dd, *J* 7.3 and 7.3, 4 × ArH), 8.17 (2 H, s, 2 × ArH), 7.94 (1 H, s, ArH), 3.75 (16 H, br, 8 × Hex-1), 3.69 (8 H, br, 4 × Hex-1), 2.71–2.63 (24 H, m, 12 × Hex-2), 2.32–2.18 (36 H, m, 12 × Me), 1.85–1.75 (24 H, m, 12 × Hex-3), 1.57–1.40 (48 H, m, 12 × Hex-4 and 12 × Hex-5), 1.51 (18 H, s, 2 × Bu^t), 1.01–0.92 (36 H, m, 12 × Hex-6), −0.31 (4 H, br, 4 × NH), −0.39 (2 H, br, 2 × NH), −0.56 (2 H, br, 2 × NH), −0.64 (2 H, br, 2 × NH), −0.79 (2 H, br, 2 × NH); *m*/*z* 2550 (calc. 2550 for $C_{177}H_{238}N_{12}O$).

Formyl-substituted tetramer 10. $\delta_H(CDCl_3$, HCl salt) 10.47 (1 H, s, CHO), 10.37 (4 H, s, 4 × mesoH), 10.33 (4 H, s, 4 × mesoH), 9.02 (4 H, s, 4 × ArH), 8.95 (8 H, br, 8 × ArH), 8.49 (4 H, dd, *J* 7.3 and 7.3, 4 × ArH), 8.16 (2 H, s, 2 × ArH), 7.95 (1 H, s, ArH), 3.77 (32 H, br, 16 × Hex-1), 2.72 (36 H, br, 12 × Me), 2.32 (44 H, br, 16 × Hex-2, 4 × Me), 1.80 (32 H, br, 16 × Hex-3), 1.60–1.10 (64 H, m, 16 × Hex-4 and 16 × Hex-5), 1.56 (18 H, s, 2 × Bu^t), 1.00–0.85 (48 H, m, 16 × Hex-6), −0.31 (8 H, br, 8 × NH), −0.40 (2 H, br, 2 × NH), −0.58 (2 H, br, 2 × NH), −0.65 (2 H, br, 2 × NH), −0.81 (2 H, br, 2 × NH), −0.79 (2 H, br, 2 × NH); *m*/*z* 3327 (calc. 3326 for $C_{231}H_{310}N_{16}O$).

Preparation of symmetric porphyrin arrays

Formyl substituted porphyrin **10** (40 mg, 12 μmol) was dissolved in CH_2Cl_2 (20 cm^3) by adding TCA (20 mg). To this mixture was added **14**[11] (2.8 mg, 12 μmol). The resulting solution was stirred at room temp. overnight under N_2 in the dark. A solution of *p*-chloranil (4.7 mg) in dry THF (0.2 cm^3) was added, and stirring was continued for another 6 h. After the usual work up, the product was separated by flash silica gel column, giving nonamer **6** (16 mg, 2.3 μmol, 38% yield based on the amount of **10** used).

Symmetric trimer porphyrin arrays **3**, **4** and **5** were prepared in essentially the same way. Use of the minimum amount of the solvents was found to lead to better yields. Symmetric porphyrin arrays **3′**, **4′** and **5′** were prepared in 17, 19 and 8% yields, respectively, using **13** instead of **14**.

Symmetric nonamer 6. $\delta_H(CDCl_3$, HCl salt) 10.41, 10.40, 10.39, 10.34 (total 18 H, br, 18 × mesoH), 9.01, 8.96 (total 32 H, br, 32 × ArH), 8.18 (4 H, s, 4 × ArH), 7.95 (2 H, s, 2 × ArH), 3.79 (64 H + 8 H, br, 32 × Hex-1 and 4 × EtC*H*$_2$Et), 2.72, 2.70 (total 96 H, br, 32 × Me), 2.27 (76 H, br, 4 × Me and 32 × Hex-2), 1.83 (64 H + 12 H, br, 32 × Hex-3 and 4 × Et-CH_3), 1.57 (36 H, br, 4 × Bu^t), 1.50–1.45 (128 H, m, 32 × Hex-4 and 32 × Hex-5), 1.00–0.96 (96 H, m, 32 × Hex-6), −0.32 (28 H, br, 28 × NH), −0.59 (4 H, br, 4 × NH), −0.82 (4 H, br, 4 × NH); δ_H([^{2}H]TFA) 10.78–10.71 (total 18 H, br, 18 × mesoH), 9.29, 9.25 (total 32 H, br, 32 × ArH), 8.33 (2 H, br, 2 × terminal-ArH), 8.31 (4 H, br, 4 × terminal-ArH), 4.03 (64 H + 8 H, br, 32 × Hex-1 and 4 × Et-CH$_2$), 2.98, 2.95 (total 96 H, br, 32 × Me), 2.51 (12 H, br, 4 × Me), 2.12 (64 H, br, 32 × Hex-2), 1.82 (64 H, br, 32 × Hex-3), 1.72 (36 H, s, 4 × Bu^t), 1.66 (12 H, br, 4 × EtCH$_3$), 1.59 (64 H, br, 32 × Hex-4), 1.49 (64 H, br, 32 × Hex-5), 1.00 (96 H, br, 32 × Hex-6); *m*/*z* 7068 (calc. 7072 for $C_{495}H_{654}N_{36}$).

Symmetric trimer 3. δ_H(CDCl$_3$) 10.46 (2 H, s, 2 × mesoH), 10.35 (4 H, s, 4 × mesoH), 8.61 (8 H, s, 8 × ArH), 7.96 (4 H, d, *J* 2.0, 4 × ArH), 7.83 (2 H, t, *J* 2.0, 2 × ArH), 4.25 (8 H, q, *J* 7.6, 4 × Et-CH$_2$), 4.16 (8 H, t, *J* 7.6, 4 × Hex-1), 4.04 (8 H, t, *J* 7.6, 4 × Hex-1), 3.25 (12 H, s, 4 × Me), 3.22 (12 H, s, 4 × Me), 2.51 (12 H, s, 4 × Me), 2.33 (8 H, m, 4 × Hex-2), 2.26 (8 H, m, 4 × Hex-2), 1.97 (12 H, t, *J* 7.6, 4 × Et-CH$_3$), 1.88 (8 H, m, 4 × Hex-3), 1.79 (8 H, m, 4 × Hex-3), 1.61–1.40 (32 H, m, 8 × Hex-4 and 8 × Hex-5), 1.54 (36 H, s, 4 × Bu^t), 0.98 (12 H, t, *J* 7.3, 4 × Hex-6), 0.94 (12 H, t, *J* 7.3, 4 × Hex-6), −1.50 (2 H, br, 2 × NH), −1.95 (4 H, br, 4 × NH); *m*/*z* 2409 (calc. 2409 for $C_{168}H_{222}N_{12}$).

Symmetric trimer 3′. δ_H([^{2}H]TFA) 10.74, 10.70 (2 H + 4 H, 2 s, 6 × mesoH), 9.23 (8 H, s, 8 × ArH), 8.33 (2 H, s, 2 × terminal-ArH), 8.30 (4 H, s, 4 × terminal-ArH), 3.99, 3.94 (16 H + 8 H, br, 2 × Hex-1), 2.93 (24 H, s, 8 × Me), 2.50 (12 H, s, 4 × Me), 2.18, 2.06 (8 H + 16 H, br, 2 × Hex-2), 1.85, 1.76 (8 H + 16 H, m, 12 × Hex-3), 1.71 (36 H, s, 4 × Bu^t), 1.6–1.4 (72 H, m, 18 × Hex-4 and 18 × Hex-5), 1.00, 0.97 (72 H, 2 t, 24 × Hex-6); *m*/*z* 2634 (calc. 2634 for $C_{184}H_{254}N_{12}$).

Symmetric pentamer 4. δ_H(CDCl$_3$, HCl salt) 10.41 (2 H, s, 2 × mesoH), 10.38 (4 H, s, 4 × mesoH), 10.34 (4 H, s, 4 × mesoH), 8.99 (8 H, s, 8 × ArH), 8.95 (8 H, 2 s, 8 × ArH), 8.17 (4 H, d, *J* 1.5, 4 × ArH), 7.95 (2 H, t, *J* 1.5, 2 × ArH), 3.90–3.62 (40 H, m, 4 × Et-CH$_2$ and 16 × Hex-1), 2.75 (12 H, s, 4 × Me), 2.72 (12 H, s, 4 × Me), 2.70 (24 H, s, 8 × Me), 2.35–2.30 (32 H, m, 12 × Hex-2), 2.27 (12 H, br, 4 × Me), 1.89 (12 H, t, *J* 7.8, 4 × Et-CH$_3$), 1.87–1.80 (32 H, m, 16 × Hex-3), 1.60 (36 H, s, 4 × Bu^t), 1.58–1.41 (64 H, m, 16 × Hex-4 and 16 × Hex-5), 1.02–0.88 (48 H, m, 16 × Hex-6), −0.32 (8 H, br, 8 × NH), −0.35 (4 H, br, 4 × NH), −0.58 (4 H, br, 4 × NH), −0.81 (4 H, br, 4 × NH); *m*/*z* 2634 (calc. 2634 for $C_{184}H_{254}N_{12}$).

Symmetric pentamer 4′. δ_H([^{2}H]TFA) 10.76, 10.75, 10.70 (total 10 H, 3 s, 10 × mesoH), 9.27, 9.23 (16 H, 2 s, 16 × ArH), 8.33 (2 H, s, 2 × terminal-ArH), 8.30 (4 H, s, 4 × terminal-ArH), 4.01, 3.94 (total 40 H, br, 20 × Hex-1), 2.96, 2.94, 2.93 (total 48 H, 3 s, 16 × Me), 2.50 (12 H, s, 4 × Me), 2.18, 2.09 (8 H + 32 H, br, 20 × Hex-2), 1.79 (40 H, m, 20 × Hex-3), 1.71 (36 H, s, 4 × Bu^t), 1.57 (40 H, m, 20 × Hex-4), 1.47 (40 H, m, 20 × Hex-5), 1.00 (60 H, m, 20 × Hex-6); *m*/*z* 4192 (calc. 4192 for $C_{292}H_{398}N_{20}$).

Symmetric heptamer 5. δ_H(CDCl$_3$, HCl salt) 10.43 (2 H, s, 2 × mesoH), 10.40 (4 H, s, 4 × mesoH), 10.38 (4 H, s, 4 × mesoH), 10.34 (4 H, s, 4 × mesoH), 9.00 (16 H, br, 16 × ArH), 8.96 (8 H, br, 8 × ArH), 8.17 (4 H, s, 4 × ArH), 7.95 (2 H, s, 2 × ArH), 3.79 (56 H, br, 24 × Hex-1 and 4 × Et-CH$_2$), 2.77–2.64 (72 H, br, 24 × Me), 2.27 (60 H, br, 24 × Hex-2 and 4 × Me), 1.90–1.73 (60 H, br, 4 × Et-CH$_3$ and 24 × Hex-3), 1.63–1.34 (96 H, br, 24 × Hex-4 and 24 × Hex-5), 1.60 (36 H, s, 4 × Bu^t), 1.02–0.90 (72 H, m, 24 × Hex-6), −0.30 (20 H, br, 20 × NH), −0.57 (4 H, br, NH), −0.80 (4 H, br, 4 × NH); *m*/*z* 5521 (calc. 5518 for $C_{384}H_{510}N_{28}$).

Symmetric heptamer 5′. δ_H([^{2}H]TFA) 10.77, 10.71 (total 14 H, br, 14 × mesoH), 9.29, 9.26 (24 H, br, 24 × ArH), 8.34 (2 H, s, 2 × terminal-ArH), 8.31 (4 H, br, 4 × terminal-ArH), 4.03 (total 56 H, br, 28 × Hex-1), 2.98, 2.96 (total 72 H, br, 24 × Me), 2.51 (12 H, br, 4 × Me), 2.12 (56 H, br, 28 × Hex-2), 1.82 (56 H, br, 28 × Hex-3), 1.72 (36 H, s, 4 × Bu^t), 1.59 (56 H, br, 28 × Hex-4), 1.49 (56 H, br, 28 × Hex-5), 1.00 (84 H, br, 24 × Hex-6); *m*/*z* 4417 (calc. 4417 for $C_{308}H_{430}N_{20}$).

Symmetric monomer 1. δ_H(CDCl$_3$) 10.22 (2 H, s, 2 × mesoH), 7.93 (4 H, s, 4 × ArH), 7.80 (2 H, s, 2 × ArH), 3.98 (8 H, m, 4 × Hex-1), 2.46 (12 H, s, 4 × Me), 2.19 (8 H, m, 4 × Hex-2), 1.73 (8 H, m, 4 × Hex-3), 1.58–1.43 (8 H, m, 4 × Hex-4), 1.50 (36 H, s, 4 × Bu^t), 1.36 (8 H, m, 4 × Hex-5), 0.90 (12 H, t, *J* 7.3, 4 × Hex-6), −2.30 (2 H, br, 2 × NH); δ_H([^{2}H]TFA) 10.63 (2 H, s, 2 × mesoH), 8.29 (2 H, s, 2 × terminal-ArH), 8.25 (4 H, s, 4 × terminal-ArH), 3.90 (8 H, t, *J* 7.6, 4 × Hex-1), 2.45 (12 H, s, 4 × Me), 2.11 (8 H, m, 4 × Hex-2), 1.79 (8 H, m, 4 × Hex-3), 1.67 (36 H, s, 4 × Bu^t), 1.56 (8 H, m, 4 × Hex-4), 1.45 (8 H, m, 4 × Hex-5), 0.97 (12 H, t, *J* 7.8, 4 × Hex-6); *m*/*z* 1080 (calc. 1079 for $C_{76}H_{110}N_4$).

Symmetric dimer 2. δ_H(CDCl$_3$) 10.34 (4 H, s, 4 × mesoH), 8.59 (4 H, s, 4 × ArH), 7.95 (4 H, d, *J* 1.8, 4 × ArH), 7.83 (2 H, t, *J* 1.8, 2 × ArH), 4.15 (8 H, t, *J* 7.8, 4 × Hex-1), 4.03 (8 H, t, *J* 7.8, 4 × Hex-1), 3.21 (12 H, s, 4 × Me), 2.50 (12 H, s, 4 × Me), 2.32 (8 H, m, 4 × Hex-2), 2.25 (8 H, m, 4 × Hex-2), 1.87 (8 H, m, 4 × Hex-3), 1.78 (8 H, m, 4 × Hex-3), 1.63–1.35 (32 H, m, 8 × Hex-4 and 8 × Hex-5), 1.53 (36 H, s, 4 × Bu^t), 0.96 (12 H, t, *J* 7.3, 4 × Hex-6), 0.93 (12 H, t, *J* 7.3, 4 × Hex-6), −1.90 (4 H, br, 4 × NH); δ_H([^{2}H]TFA) 10.72 (2 H, s, 2 × mesoH), 9.20 (4 H, s, 4 × ArH), 8.34 (2 H, s, 2 × terminal-ArH), 8.30 (4 H, s, 4 × terminal-ArH), 3.99, 3.93 (8 H + 8 H, m, 8 × Hex-1), 2.91 (12 H, s, 4 × Me), 2.50 (12 H, s, 4 × Me), 2.18, 2.03 (8 H + 8 H, m, 8 × Hex-2), 1.84, 1.74 (8 H + 8 H, m, 8 × Hex-3), 1.71 (36 H, s, 4 × Bu^t), 1.59, 1.53 (8 H + 8 H, m, 8 × Hex-4), 1.48, 1.47 (8 H + 8 H, m, 8 × Hex-5), 0.99, 0.96 (12 H + 12 H, 2 t, *J* 6.7 and 6.7, 8 × Hex-6); *m*/*z* 1857 (calc. 1856 for $C_{130}H_{182}N_8$).

Acknowledgements

This work was supported by Grant-in-Aids (No. 02101005 and 07228232) from the Ministry of Education, Science and Culture of Japan.

References

1 G. McDermott, S. M. Prince, A. A. Freer, A. M. Hawthornwaite-Lawless, M. Z. Papiz, R. J. Cogdell and N. W. Isaaca, *Nature*, 1995, **374**, 517.
2 M. R. Wasielewski, *Chem. Rev.*, 1992, **92**, 435.
3 (*a*) A. Osuka, K. Ida and K. Maruyama, *Chem. Lett.*, 1989, 741; (*b*) T. Nagata, A. Osuka and K. Maruyama, *J. Am. Chem. Soc.*, 1990, **112**, 3054; (*c*) A. Osuka, T. Nagata and K. Maruyama, *Chem. Lett.*, 1991, 481; (*d*) A. Osuka, B. Liu and K. Maruyama, *Chem. Lett.*, 1993, 949.
4 A preliminary communication of this work; A. Osuka, N. Tanabe, R.-P. Zhang and K. Maruyama, *Chem. Lett.*, 1993, 1505.
5 L. R. Milgrom, *J. Chem. Soc., Perkin Trans. 1*, 1983, 2535; J. Dalia, A. Harriman and L. R. Milgrom, *Chem. Phys. Lett.*, 1987, **136**, 427; O. Wennerstrom, H. Ericsson, I. Ratson, S. Svensson and W. Pimlott, *Tetrahedron Lett.*, 1989, **30**, 1129.
6 H. L. Anderson and J. K. M. Sanders, *J. Chem. Soc., Chem. Commun.*, 1989, 1714; S. Anderson, H. L. Anderson and J. K. M. Sanders, *Angew. Chem., Int. Ed. Engl.*, 1992, **31**, 907; G. M. Dubowchik and A. D. Hamilton, *J. Chem. Soc., Chem. Commun.*, 1987, 293; M. J. Crossley and P. L. Burn, *J. Chem. Soc., Chem. Commun.*, 1991, 1569; S. Anderson, H. L. Anderson, A. Bashall, M. McPartlin and J. K. M. Sanders, *Angew. Chem., Int. Ed. Engl.*, 1995, **34**, 1096.
7 (*a*) J. L. Sessler and V. L. Capuano, *Angew. Chem., Int. Ed. Engl.*, 1990, **29**, 1134; (*b*) J. L. Sessler, V. L. Capuano and A. Harriman, *J. Am. Chem. Soc.*, 1993, **115**, 4618.
8 S. Prathapan, T. E. Johnson and J. S. Lindsey, *J. Am. Chem. Soc.*, 1993, **115**, 5719; R. W. Wagner and J. S. Lindsey, *J. Am. Chem. Soc.*, 1994, **116**, 9759.
9 3,5-Di-*tert*-butylphenyl substituent has been often employed in artificial models, since its introduction gives porphyrins good solubility in common organic solvents by blocking π–π-stacking of porphyrins. See: S. Noblat, C. O. Dietrich-Buchecker and J.-P. Sauvage, *Tetrahedron Lett.*, 1987, **28**, 5829.
10 T. Nagata, *Bull. Chem. Soc. Jpn.*, 1991, **64**, 3005.
11 P. S. Clezy and A. W. Nichol, *Aust. J. Chem.*, 1965, **11**, 1835.
12 M. Kasha, H. R. Rawls and M. A. El-Bayoumi, *Pure Appl. Chem.*, 1965, **11**, 371.

Paper 5/04801J
Received 21*st July* 1995
Accepted 1*st September* 1995